**Research article** Rapports De Pharmacie Vol.3 (4), 2017, 413-422
ISSN: 2455-0507

# DEVELOPMENT AND CHARACTERIZATION OF PROMISING NANOPARTICULATE DRUG DELIVERY SYSTEMS CONTAINING QUERCETIN

**Koh Yik Sin, Jaya Raja Kumar**

[1]*Research student, Asian Institute of Medicine, Science and Technology (AIMST) University, Bedong 08100, Kedah, Malaysia*

[2]*Unit of Pharmaceutical Technology, Faculty of Pharmacy, Asian Institute of Medicine, Science and Technology (AIMST) University, Bedong 08100, Kedah, Malaysia*

**ABSTRACT**

Quercetin is a flavonol compound that is well-known for its antioxidant and anti-inflammatory properties, hence, it is widely used in the treatment and prevention of many diseases and cancers. In order to improve its solubility and bioavailability, the aim of this study was to prepare quercetin loaded PLGA nanoparticles by using single emulsion solvent evaporation method. PLGA is chosen as the polymer in this formulation due to its safety profile, easy processing, biodegradable and biocompatible nature. Seventeen runs of quercetin nanoparticles were prepared according to the variation in amount of quercetin, PLGA polymer and percentage of PVA solution. The variables such as particle size, polydispersity index, entrapment efficiency and cumulative drug release after 24 hr were determined as the responses for the formulations. Fourier transform infra-red (FT-IR) spectroscopy and scanning electron microscopy were employed to characterize quercetin nanoparticles.

**Keywords:** Quercetin nanoparticles, PLGA, PVA, Particle size, Probe sonication

## INTRODUCTION

Quercetin is a flavonol which categorized under the subclass of flavonoids that is commonly found in fruits and vegetables such as cranberries, blueberries, kale, celery, broccoli, red grapes, tomatoes and onions [1,2]. The chemical name of quercetin is 2- (3, 4-dihydroxyphenyl)-3,5,7-trihydroxy-4H-1-benzopyran-4-one [3]. As quercetin is well-known for its antioxidant and anti-inflammatory properties, thus, it is widely used in the treatment and prevention of many diseases and cancers. These include pancreatitis, prostatitis, coronary artery, asthma as well as helps in reducing the diabetic complications. The antioxidant activity of quercetin is mainly due to its ability to scavenge free radicals present in the body and bind to transition metal ions [2].

Several studies has shown that quercetin has anticancer property which inhibiting the growth of cancerous cells in breast, prostate, colon, lungs, liver and brain by the mechanism of antioxidant activity. Quercetin helps in decreasing the reactive oxygen species induced DNA damage, inhibition of the proliferation of cancer cells, promoting apoptosis and blocking of cell cycle. Other than that, quercetin also has anti-inflammatory action which reduces the inflammatory mediators such as prostaglandins and leukotrienes that are responsible for causing pain and inflammation in human body. In this case, quercetin acts by inhibiting the cyclooxygenase as well as lipoxygenase enzymes that accountable for the production of prostaglandins and leukotrienes [2]. However, quercetin is proved too has very poor oral bioavailability that resulting from its poor permeability and low water solubility. This drawback created a big challenge in the delivery and absorption of quercetin [3]. In order to solve this problem, quercetin can be formulated as polymeric nanoparticles which act as controlled-released drug delivery for better therapeutic performance. Polymeric nanoparticles are extensively used in advanced dosage form development because they have good stability, higher encapsulation efficiency and permit the control release of the encapsulated hydrophobic drugs at the target site to enhance the solubility lead to a better bioavailability [3]. Nanoparticles are a class of particulate matters which have a size ranging from 1-1000nm and they are recently been discovered to apply in many fields such as biomedical, manufacturing and materials, engineering as well as environmental aspects [4] Moreover, formulation of drugs as nanoparticles helps to protect them from degradation by gastric juice and undesired environment, enhances the solubility as well as serves as drug targeting [5].

**Address for correspondence:**
Koh Yik Sin,
Research student,
AIMST University,Bedong- Semeling, Kedah,
Malaysia 08100

For the formulation of polymeric nanoparticles, there are some requirements to be considered for selection of an appropriate and ideal polymer which included drug loading capability, mechanical strength, stability profile, toxicological profile as well as biodegradation strength [6]. One of the widely use synthetic polymers is Poly (lactic-co-glycolic acid) (PLGA) polymer that are being used by many researchers for the development of new products or techniques in various types of aspects. PLGA is being approved by Food and Drug Administration (FDA) because of its biodegradable, biocompatible and non-toxic properties. For the reason of its safety and easy processing, PLGA is generally applied in the synthesis of microparticles or nanoparticles especially for those hydrophobic and potent drugs to be delivered in a controlled manner and to the specific tissues of the body for better therapeutic efficacy. Basically, the synthesized nanoparticles can consider to be administered in various ways such as oral, topical, nasal, ophthalmic and parenteral delivery which depends on the purposes and therapeutic uses of the formulation [5].

PLGA is broadly chosen as the drugs carrier for the synthesis of nanoparticles in controlled- released drug delivery system and cell targeting action amongst many synthetic polymers. PLGA has great potential in medicine applications as it is biocompatible in human body, non-toxic, able to control the release of drug for prolonged residence time and useful in targeted drug delivery such as delivering particular drug to the specific cancer site [7]. In this paper, quercetin loaded PLGA nanoparticles were prepared by using solvent evaporation technique. Polymer solutions were prepared in volatile solvents in order to produce emulsions by using polyvinyl alcohol (PVA) as emulsifying agent or surfactant. The emulsion formed was then subjected to evaporation of organic solvent to form rigid nanoparticles [8].

## EXPERIMENTAL

### Materials:

Quercetin was obtained from Sigma-Aldrich Co., Poly(lactic-co-glycolic acid) PLGA with the molecular weight of 38000-54000 was purchased from Sigma-Aldrich Co., Dichloromethane (DCM) was purchased from RCI Labscan, polyvinyl alcohol (PVA) were purchased from R&M Marketing, Essex, U.K., Dimethyl sulfoxide (DMSO) was purchased from Fisher Chemical, U.K., Potassium bromide was obtained from Nacalai Tesque, Kyoto, Japan. All the chemicals and solvents used in this research were of analytical grade.

## METHODS OF PREPARATION

*Preparation of quercetin-loaded PLGA nanoparticles:*

Quercetin-loaded PLGA nanoparticles were prepared by single emulsion solvent evaporation technique. The nanoparticles were synthesized by using various concentrations of quercetin, PLGA and PVA solution. Initially, the required amount of quercetin and PLGA polymer were accurately weighed by using an electronic balance. The weighed quercetin and PLGA polymer were dissolved in 2ml of DCM solvent separately. Drug solution was added to polymer solution and allowed for mixing by using vortex mixer. 1ml of Dimethyl sulfoxide (DMSO) was then added to the drug-polymer solution to completely dissolve the quercetin drug. Quercetin-PLGA solution served as dispersed phase was added drop by drop to the PVA solution. The resultant emulsion was immediately sonicated at 55Hz power for 5 min using a probe sonicator (Qsonica Q55 Sonicator, USA). The prepared emulsion was left on a magnetic stirrer at 1000 rpm and 70°C for 1 hour, so that its organic solvents would evaporate and diffuse and as a result nanoparticles would form. To separate the nanoparticles from the continuous phase and residual solvent, first, Quercetin-PLGA nanoparticles were centrifuged (Beckman Coulter Avanti J-26S XPI centrifuges) at 14,100g and 10°C for 30 min, and the supernatant was discarded. The quercetin-PLGA nanoparticles were washed 1 more time. Finally, the sample was lyophilized in (Thermo Scientific-SuperModulyo 230, USA).

## IN VITRO EVALUATION STUDIES

*Measurement of Particle size and Polydispersity Index (PDI):*

The mean particle size and PDI of each formulation were established by using particle size analyzer (Anton Paar Malaysia - Litesizer 500). The polymeric nanoparticle were diluted with water (0.8903 mPa.s), sonicated for 10 min and filtered. The samples of nanoparticles were transferred to plastic cuvette and subjected for the measurement of particle size and PDI at 25 °C with an angle of detection is automatic. Number of runs 60 and measurement time 0h 00m 10s. [3]

*Determination of Entrapment efficiency (EE):*

The entrapment efficiency of quercetin nanoparticles was determined by centrifugation of the colloidal samples at 15000 rpm at 25 °C for 15 min. The

amount of quercetin entrapped within nanoparticles was calculated by difference between the total amount of drug used and the amount present in the aqueous phase of supernatant. The non-entrapped quercetin in the supernatant obtained after ultracentrifugation of nanoparticles was determined by HPLC method at 354 nm. The % EE was then calculated by mass ratio of the encapsulated drug to the amount of drug initially added in formulation. The EE was determined using the following equation:

*% Entrapment = W–w/W*100*,

Where, W = theoretical amount of quercetin; w = observed amount of quercetin. [3]

*In vitro drug release:*

In vitro release of quercetin-loaded PLGA nanoparticles were performed by suspending 10 mg of equivalent quercetin in 10 ml of phosphate buffer (pH 7.4) in a 50 ml volumetric flask and incubated at 37 °C with shaking at 100 rpm in orbital shaker (ERLA -ES203D). At predetermined time intervals, 2 mL release medium was taken out from flask and replaced with 2 mL fresh phosphate buffer to keep the volume constant. The concentration of drug in the medium was deter-mined by using HPLC method. Subsequently, the percentage of cumulative drug released was obtained after 12 hours.[3]

RP HPLC chromatographic separation was performed on a Shimadzu liquid chromatographic system equipped with a LC-20AD solvent delivery system (pump), SPD-20A photo diode array detector, and SIL-20ACHT injector with 50µL loop volume. The LC solution version 1.25 was used for data collecting and processing (Shimadzu, Japan). The HPLC was carried out at a flow rate of 1.0 ml/min using a mobile that is phase constituted of acetonitrile, 20mm AA: 5.5% ACN (pH 4.5) (20:80, v/v), and detection was made at 354nm. The mobile phase was prepared daily, filtered through a 0.45µm membrane filter (Millipore) and sonicated before use. A Thermo C18 column (25cm × 4.6mm i.d., 5µ) was used for the separation.

*FTIR spectral studies:*

The Fourier transform infrared (FTIR) spectra for free drug, free PLGA, quercetin-loaded PLGA nanoparticles and physical mixture of quercetin and PLGA were obtained from FTIR spectrophotometer IR (Perkin Elmer, Germany) for characterization of the chemical integrity of quercetin inside PLGA nanoparticles. In summary, the specimens pressed with potassium bromide (KBr) to make a pellet by applying a pressure of 100 kg/cm$^2$ before obtaining their IR absorption spectra. The spectra were detected in KBr discs over a range of 4000–400 cm−1.

## RESULT AND DISCUSSION

In this paper, we had obtained the successful effect on the formulation of quercetin nanoparticles. Through preliminary tests, the Drug (A), PLGA polymer (B) and PVA solution (C) were identified as the most significant variables that affecting four responses which including particle size, polydispersity index, entrapment efficiency and % CDR . Among various design approaches, the Box-Behnken (BBD) shows good design properties, which was commonly used to evaluate the main effects and interaction effects on different responses. It was used when region of interest and region of operability nearly the same. This Box-Behnken design is suitable for determining the quadratic response surfaces and constructing second order polynomial models. The BBD consists of simulated center points and the set of points lying at the midpoint of each edge of the multi-dimensional cube.

Seventeen runs were essential for the response surface methodology based on the BBD. Based on the experimental design, the combination of several factors produced different responses as presented in Table 1. These results clearly point out that all the dependent variables are strongly dependent on the selected independent variables as they show a wide variation among the 17 runs. Data were analyzed using Stat-Ease Design-Expert software (DX11) to obtain analysis of variance (ANOVA), regression coefficients and regression equation. Mathematical relationship was produced using multiple linear regression analysis for the studied variables are expressed as shown in Table 2.

**Table-2: Regression equation for the response**

| Response | Regression equation |
|---|---|
| **R1** | = +253.14+3.63A+2.62B-0.2800C-0.1975AB+0.4575AC-0.7775BC+2.80A²+0.8002B²+0.1003C² |
| **R2** | =+0.1246+0.0214A+0.0383B+0.0096C-0.0188AB-.0260AC+0.0167BC+0.0312A²+0.1270B²+0.0407C² |
| **R3** | = +68.61+1.20A+4.72B+0.0150C-0.0875AB+1.02AC+0.2950BC+0.3817 A²+1.31B²+0.2943C² |
| **R4** | = +56.55+0.1575A+4.20B+0.1363C+0.2325AB+0.0575AC-0.0100BC+0.2400A²-0.4825B²-0.1375C² |

**Table-1: Factorial design of quercetin nanoparticles formulations**

| Run | Factor 1 A:Quercetin (mg) | Factor 2 B: PLGA (mg) | Factor 3 C: PVA solution (%) | R-1 Particle size (nm) | R- 2 Polydispersity index | R-3 Entrapment efficiency (%) | R- 4 CDR after 24 hour (%) |
|---|---|---|---|---|---|---|---|
| 1 | 15 | 100 | 1 | 259.51 | 0.321 | 74.12 | 60.12 |
| 2 | 10 | 100 | 2 | 254.61 | 0.312 | 73.38 | 60.01 |
| 3 | 20 | 75 | 1 | 258.02 | 0.224 | 69.13 | 56.43 |
| 4 | 10 | 75 | 3 | 253.14 | 0.221 | 67.4 | 56.76 |
| 5 | 15 | 75 | 2 | 252.71 | 0.121 | 68.11 | 56.36 |
| 6 | 10 | 50 | 2 | 250.61 | 0.211 | 63.47 | 52.11 |
| 7 | 15 | 50 | 1 | 251.09 | 0.265 | 65.55 | 51.66 |
| 8 | 15 | 75 | 2 | 253.14 | 0.129 | 68.36 | 56.13 |
| 9 | 10 | 75 | 1 | 252.66 | 0.129 | 70.16 | 56.41 |
| 10 | 15 | 100 | 3 | 255.44 | 0.353 | 75.48 | 60.18 |
| 11 | 15 | 50 | 3 | 250.13 | 0.23 | 65.73 | 51.76 |
| 12 | 15 | 75 | 2 | 252.61 | 0.127 | 68.79 | 56.54 |
| 13 | 20 | 50 | 2 | 259.26 | 0.291 | 67.41 | 52.14 |
| 14 | 15 | 75 | 2 | 253.17 | 0.122 | 68.66 | 56.96 |
| 15 | 20 | 75 | 3 | 260.33 | 0.212 | 70.47 | 57.01 |
| 16 | 20 | 100 | 2 | 262.47 | 0.317 | 76.97 | 60.97 |
| 17 | 15 | 75 | 2 | 254.08 | 0.124 | 69.15 | 56.76 |

**Table-3: ANOVA results of the quadratic model for the response of particle size (R1)**

| Source variations | Sum of Squares | DF | Mean Square | F Value | p-value Prob>F | |
|---|---|---|---|---|---|---|
| **Model** | 201.48 | 9 | 22.39 | 9.63 | 0.0034 | significant |
| **A-Quercetin** | 105.56 | 1 | 105.56 | 45.42 | 0.0003 | |
| **B-PLGA** | 54.81 | 1 | 54.81 | 23.58 | 0.0018 | |
| **C- PVA solution** | 0.6272 | 1 | 0.6272 | 0.2699 | 0.6194 | |
| **AB** | 0.1560 | 1 | 0.1560 | 0.0671 | 0.8030 | |
| **AC** | 0.8372 | 1 | 0.8372 | 0.3602 | 0.5673 | |
| **BC** | 2.42 | 1 | 2.42 | 1.04 | 0.3417 | |
| **$A^2$** | 32.90 | 1 | 32.90 | 14.16 | 0.0071 | |
| **$B^2$** | 2.70 | 1 | 2.70 | 1.16 | 0.3171 | |
| **$C^2$** | 0.0423 | 1 | 0.0423 | 0.0182 | 0.8965 | |
| **Residual** | 16.27 | 7 | 2.32 | | | |

**Table-4: ANOVA results of the quadratic model for the response of polydispersity index (R2)**

| Source variations | Sum of Squares | DF | Mean Square | F Value | p-value | |
|---|---|---|---|---|---|---|
| **Model** | 0.1056 | 9 | 0.0117 | 66.01 | < 0.0001 | significant |
| **A-Quercetin** | 0.0037 | 1 | 0.0037 | 20.56 | 0.0027 | |
| **B-PLGA** | 0.0117 | 1 | 0.0117 | 65.84 | < 0.0001 | |
| **C-PVA solution** | 0.0007 | 1 | 0.0007 | 4.17 | 0.0805 | |
| **AB** | 0.0014 | 1 | 0.0014 | 7.91 | 0.0261 | |
| **AC** | 0.0027 | 1 | 0.0027 | 15.21 | 0.0059 | |
| **BC** | 0.0011 | 1 | 0.0011 | 6.31 | 0.0402 | |
| **$A^2$** | 0.0041 | 1 | 0.0041 | 23.06 | 0.0020 | |
| **$B^2$** | 0.0679 | 1 | 0.0679 | 381.70 | < 0.0001 | |
| **$C^2$** | 0.0070 | 1 | 0.0070 | 39.23 | 0.0004 | |
| **Residual** | 0.0012 | 7 | 0.0002 | | | |

**Table-5: ANOVA results of the quadratic model for the response of entrapment efficiency (R3)**

| Source variations | Sum of Squares | DF | Mean Square | F Value | p-value | |
|---|---|---|---|---|---|---|
| **Model** | 203.28 | 9 | 22.59 | 27.90 | 0.0001 | significant |
| **A-Drug** | 11.45 | 1 | 11.45 | 14.14 | 0.0071 | |
| **B-Tween 20** | 178.51 | 1 | 178.51 | 220.50 | < 0.0001 | |
| **C-Span 20** | 0.0018 | 1 | 0.0018 | 0.0022 | 0.9637 | |
| **AB** | 0.0306 | 1 | 0.0306 | 0.0378 | 0.8513 | |
| **AC** | 4.20 | 1 | 4.20 | 5.19 | 0.0568 | |
| **BC** | 0.3481 | 1 | 0.3481 | 0.4300 | 0.5329 | |
| **$A^2$** | 0.6136 | 1 | 0.6136 | 0.7580 | 0.4128 | |
| **$B^2$** | 7.25 | 1 | 7.25 | 8.95 | 0.0202 | |
| **$C^2$** | 0.3646 | 1 | 0.3646 | 0.4503 | 0.5237 | |
| **Residual** | 5.67 | 7 | 0.8096 | | | |

**Table-6: ANOVA results of the quadratic model for the response of CDR after 24 hours (R4)**

| Source variations | Sum of Squares | DF | Mean Square | F Value | p-value | |
|---|---|---|---|---|---|---|
| **Model** | 143.05 | 9 | 15.89 | 196.40 | < 0.0001 | significant |
| **A-Quercetin** | 0.1985 | 1 | 0.1985 | 2.45 | 0.1614 | |
| **B-PLGA** | 141.20 | 1 | 141.20 | 1744.72 | <0.0001 | |
| **C-PVA solution** | 0.1485 | 1 | 0.1485 | 1.84 | 0.2176 | |
| **AB** | 0.2162 | 1 | 0.2162 | 2.67 | 0.1462 | |
| **AC** | 0.0132 | 1 | 0.0132 | 0.1634 | 0.6981 | |
| **BC** | 0.0004 | 1 | 0.0004 | 0.0049 | 0.9459 | |
| **$A^2$** | 0.2425 | 1 | 0.2425 | 3.00 | 0.1270 | |
| **$B^2$** | 0.9802 | 1 | 0.9802 | 12.11 | 0.0103 | |
| **$C^2$** | 0.0796 | 1 | 0.0796 | 0.9836 | 0.3543 | |
| **Residual** | 0.5665 | 7 | 0.0809 | | | |

The normality of the data could be established through the normal % probability plot of the externally studentized residuals. If the points on the plot lie on a straight line, the residuals are normally distributed as shown in (Figure 1a,b,c and d).

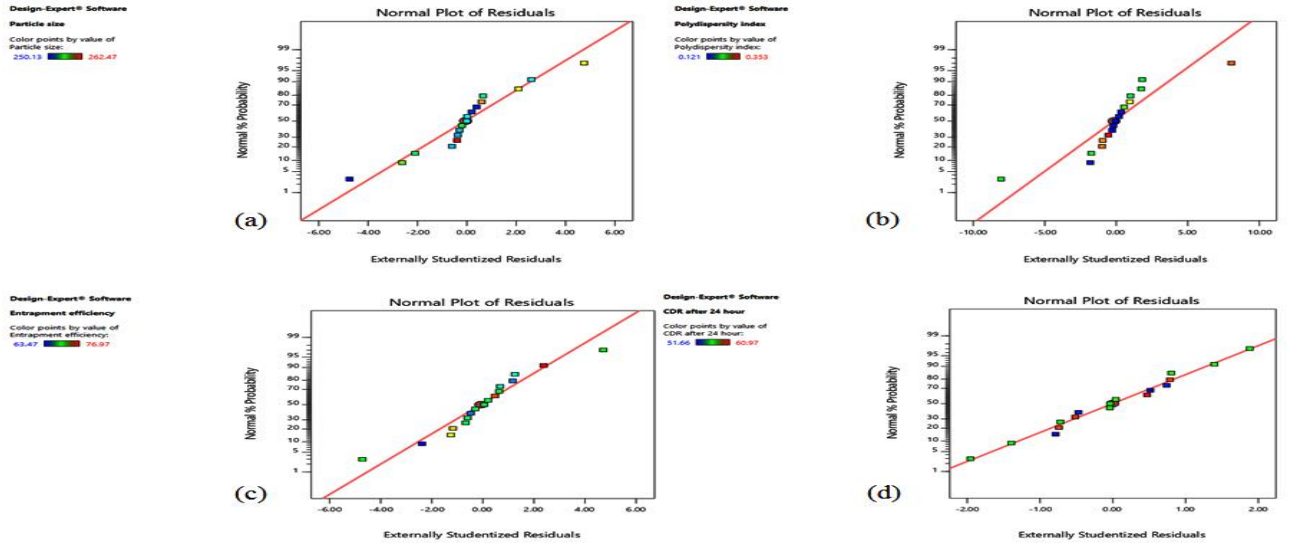


**Figure-1: (a) Normal plot of the externally studentized residuals on particle size (R1). (b) Normal plot of the externally studentized residuals on polydispersity index (R2). (c) Normal plot of the externally studentized residuals on entrapment efficiency (R3). (d) Normal plot of the externally studentized residuals on CDR after 24 hours (R4).**

The assumption of constant variance was tested by plotting externally studentized residual against predicted values as illustrated in the figures below (Figure 5-8) which showing the results of different responses (R1-R4). The studentized residuals are located by dividing the residuals by their standard deviations. Based on the evident from (Figure 2a,b,c and d), the points are scattered randomly between the outlier detection limits - 4.82 to + 4.82.

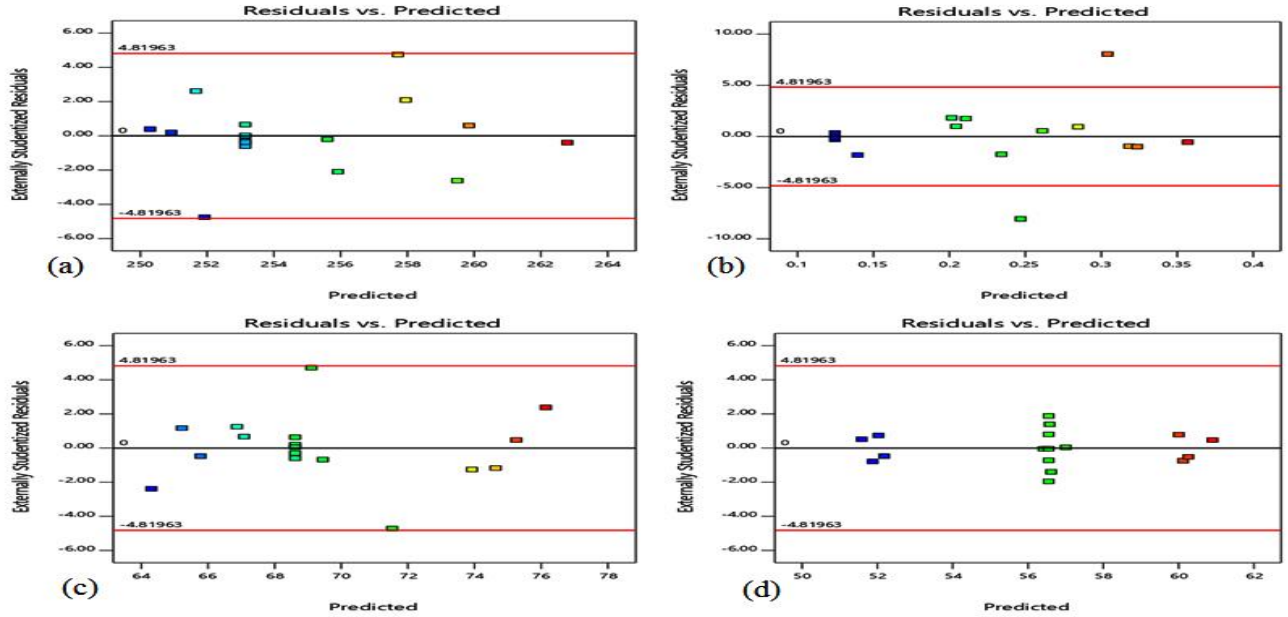


**Figure-2: (a) Residuals vs. Predicted (R1). (b) Residuals vs. Predicted (R2). (c) Residuals vs. Predicted (R3). (d) Residuals vs. Predicted (R4).**

The graphs showed that Residuals vs. Predicted and Residuals vs. Run were scattered randomly. From the results, it can therefore be seen that the model is considered suitable for use and can be used to identify the optimal parameters. The response R1, R2, R3 and R4 results showed in (Figure 3a,b,c and d ) were quite satisfactory, while R2 result was considered accepted. Still, a high correlation between observed and predicted data shown indicates their low discrepancies.

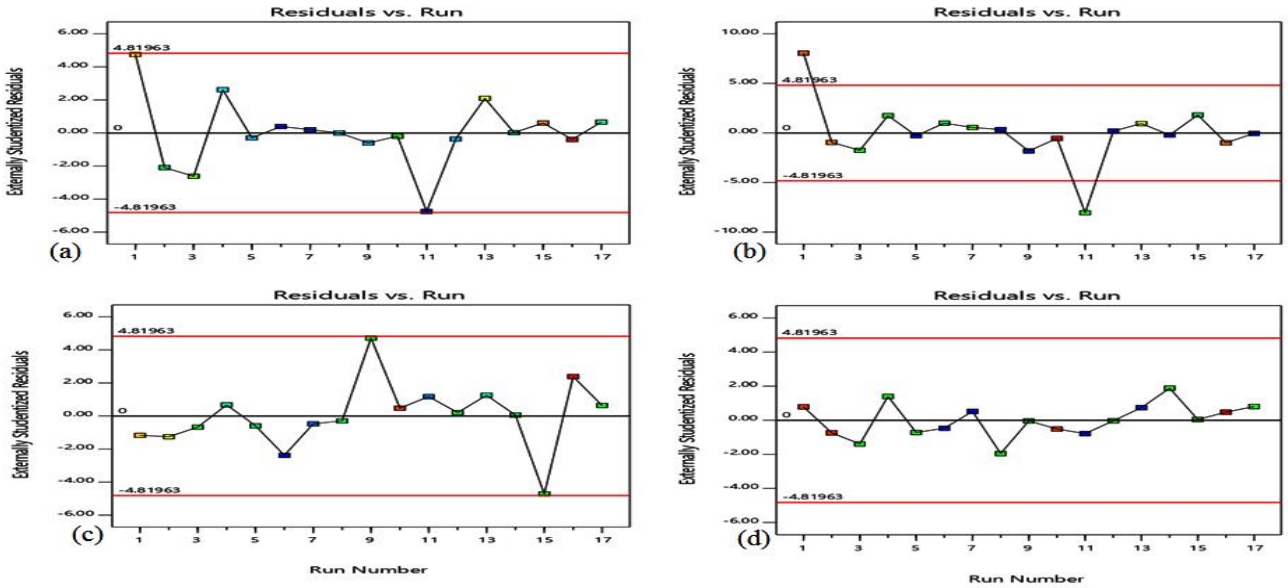


**Figure-3:(a) Residuals vs. Run (R1). (b) Residuals vs. Run (R2). (c) Residuals vs. Run (R3). (d) Residuals vs. Run (R4)**

The transformation parameter, λ, is chosen such that it maximizes the log-likelihood function. The maximum likelihood estimate of λ agrees to the value for which the squared sum of errors from the fitted model is a minimum. This value of λ is determined by fitting a numerous values of λ and choosing the value corresponding to the minimum squared sum of errors. t can also be chosen graphically from the Box-Cox normality plot. Value of λ = 1.00 indicates that no transformation needed and produces results identical to original data shown in (Figure 4a,b,c and d).

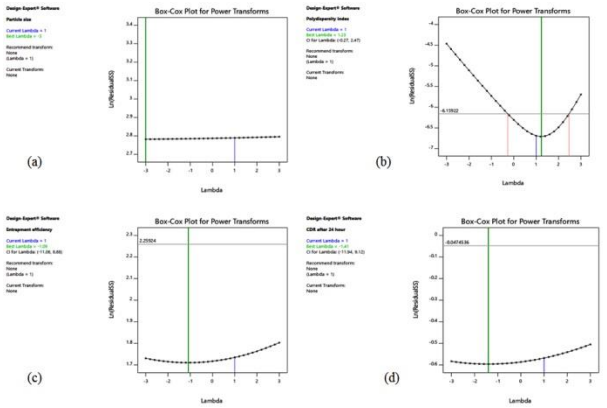


**Figure-4: (a) Box-Cox Plot (R1). (b) Box-Cox Plot (R2). (c) Box-Cox Plot (R3). (d) Box-Cox Plot (R4).**

A particle size of quercetin nanoparticles was found to be in the range of 250.13 – 262.47 nm as shown in Table 1. The factorial equation for particle size exhibited a good correlation coefficient (1.000) and the Model F value of 9.63 which implies the model is significant. P-values less than 0.0500 indicate model terms are significant. Values greater than 0.1000 indicate the model terms are not significant. In this case A, B and $A^2$ are significant model shown in Table 3. The influence of the main and interactive effects of independent variables on the particle size was further elucidated using the perturbation and 3D response surface plots. The individual main effects of A, B and C on particle size are as shown in Figure 5a. This figure clearly showed that A has the major effect on R1 whereas B and C have little effects on R1.The 2D contour plots and the 3D response surfaces of the response R1 are shown in (Figure 5b and c) to depict the interactive effects of independent variables on response R1, one variable was kept constant whereas the other two variables diverse in a certain range. The shapes of response surfaces and contour plots reveal the nature and extent of the interaction between different factors. The interaction between A and B on particle size and size distribution is shown in (Figure 5e and d). At low levels of A, R1 obtained from 252.66 to 254.61nm. Similarly at high levels of A, R1 obtained from 258.02 to 262.47nm.

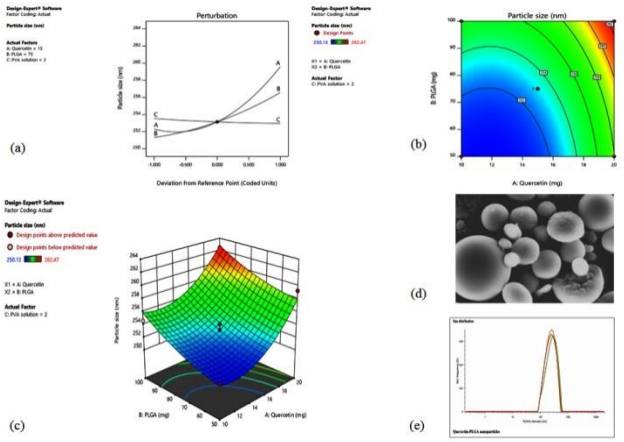


**Figure-5: (a) Perturbation plot showing the main effect of Quercetin (A), PLGA (B) and PVA solution (C) on Particle size (R1). (b) Response surface plot presenting the interaction between the drug and PLGA affecting the particle size (R1) of nanoparticles. (c) 3D Response surface plot presenting the interaction between the drug and PLGA affecting the particle size (R1) of nanoparticles. (d) SEM photography of quercetin-loaded PLGA nanoparticles. (e) Particle size analysis of quercetin nanoparticles.**

The coefficient of determination, R-squared, is a measure of the fraction of the total squared error that is explained by the model. By definition the value of $R^2$ varies between zero and one and the closer it is to one, the better. However, a large value of $R^2$ does not necessarily imply that the regression model is good one. Adding a variable to the model will always increase $R^2$, regardless of whether the additional variable is statistically significant or not. Thus it is possible for models that have large values of $R^2$ to CDR poor predictions of new observations or estimates of the mean response. To avoid this confusion, an extra statistic called the Adjusted R-squared statistic is needed; its value decreases if unnecessary terms are added. These two statistics can, when used together, imply the existence of extraneous terms in the computed model which is indicated by a large difference, usually of more than 0.20, between the values of $R^2$ and Adj-$R^2$. The amount by which the output predicted by the model differs from the actual output is called the residual. Predicted Residual Error Sum of Squares (PRESS) is

a measure of how the model fits each point in the design. It is used to calculate predicted $R^2$. Adeq Precision measures the signal to noise ratio. A ratio greater than 4 is desirable. "Adeq precision" showed (R1, R2, R3, R4) was 10.691, 22.714, 17.157 and 42.698 indicates an adequate signal respectively. This model can be used to navigate the design space. These statistics are used to prevent over fitting of model. Subsequently producing the polynomial equations relating the dependent and independent variables, the process was optimized for the responses as shown in Table 2.

The mathematical model generated for polydispersity index (R2) was found to be significant with F-value of 66.01 ($p < 0.0001$) and $R^2$ value of 0.9884. There is only a 0.01% chance that an F-value this large could occur due to noise. The variables A, B, AB, AC, BC, $A^2$, $B^2$, $C^2$ have significant effects on the polydispersity index, since the P-values obtained were less than 0.0500 indicate the significant model terms as shown in Table 4. The influence of the main and interactive effects of independent variables on the polydispersity index was further elucidated using the perturbation and 3D response surface plots. The perturbation plot (Figure 6a) showing the main effects of A, B and C on the polydispersity index (R2) of quercetin nanoparticles. This figure clearly shows that B has the main and the major effect on R2 followed by C which has a little effect on R2. The relationship between the dependent and independent variables was further elucidated using 2D and 3D response surface plots are shown in (Figure 6b and 6c). Figure 6a shows the interactive effect of A and B on the polydispersity index (R2). At low levels of A (Drug), R2 gives the values from 0.129 to 0.312. On the other hand, at high levels of A, R2 values range from 0.212 to 0.317.

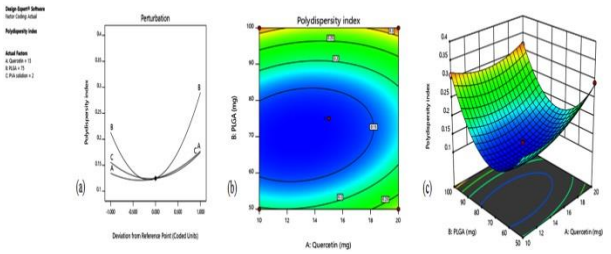


**Figure-6: (a) Perturbation plot showing the main effect of Drug (A), PLGA (B) and PVA solution (C) on polydispersity index (R2). (b) 2D-Response surface plot presenting the interaction between the drug and PLGA affecting the polydispersity index (R2). (c) 3D-Response surface plot presenting the interaction between the drug and PLGA affecting the polydispersity index (R2).**

The accurate model produced for entrapment efficiency (R3) was found to be significant with F-value of 27.90 ($p < 0.0001$) and $R^2$ value of 0.9729. The independent variables A, B, C has significant effects on the entrapment efficiency (R3), since the P-values less than 0.0500 represent the significant model terms as shown in Table 5. In this model A, B, $B^2$ are significant model terms. The perturbation plot (Figure 7a) showing the main effects of A, B and C on the entrapment efficiency (R3) of quercetin nanoparticles. It is found that the quantity of PLGA (B) has the major effect on affecting the entrapment efficiency (R3) of nanoparticles while A and C have less effect on R3. The correlation among the dependent and independent variables was further elucidated using 2D and 3D response surface plots are shown in (Figure 7b and 7c). Figure 25 shows the interactive effect of A and B on the entrapment efficiency (R3) at fixed level of C. At low levels of A (Drug), R3 increases from 63.47% to 73.38%.On the other hand, at high levels of A, R3 increases from 67.41% to 76.97%.

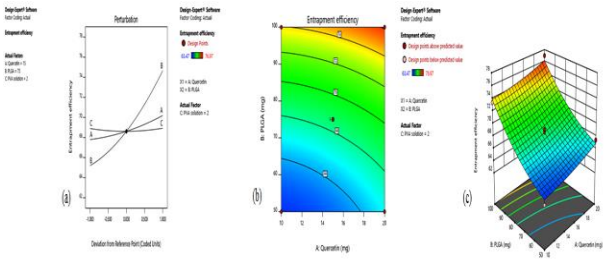


**Figure-7: (a) Perturbation plot showing the main effect of Drug (A), PLGA (B) and PVA solution (C) on entrapment efficiency (R3). (b) Response surface plot presenting the interaction between the drug and PLGA affecting the entrapment efficiency (R3). (c) Response surface plot presenting the interaction between the drug and PLGA affecting the entrapment efficiency (R3).**

The accurate model produced for %CDR after 24 hours (R4) was found to be significant with F-value of 196.40 ($p < 0.0001$) and $R^2$ value of 0.9961. Since the P-values less than 0.0500 represent the model terms are significant. In this model B and $B^2$are significant model which shown in Table 6. The perturbation plot (Figure 8a) showing the main effects of A, B and C on the %CDR after 24 hours (R4) of quercetin nanoparticles. The correlation

among the dependent and independent variables was further elucidated using 2D and 3D response surface plots are shown in (Figure 8b and 8c). Figure 8a shows the interactive effect of A and B on the %CDR after 24 hours (R4) at fixed level of C. At low levels of A (Drug), R4 gives the values range from 52.11% to 60.01%.On the other hand, at high levels of A, R4 gives the values range from 52.14% to 60.97%.

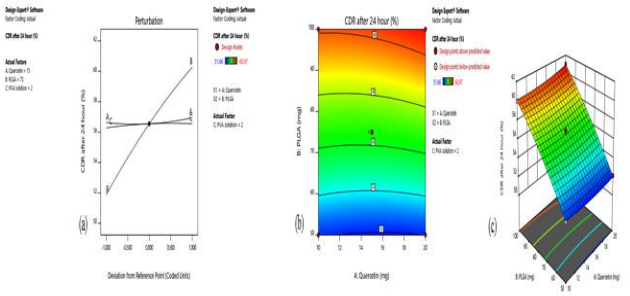

**Figure-8: (a) Perturbation plot showing the main effect of Drug (A), PLGA (B) and PVA solution (C) on CDR after 24 hours (R4). (b) Response surface plot presenting the interaction between the drug (A) and PLGA (B) affecting CDR after 24 hours (R4). (c) Response surface plot presenting the interaction between the drug (A) and PLGA (B) affecting CDR after 24 hours (R4).**

Numerical optimization using the desirability approach was employed to locate the optimal settings of the process variables to achieve the desired responses. Q5, Q8 and Q14 batch codes of quercetin nanoparticles were fabricated and measured according to these optimized levels for further evaluation of the responses. The observed values of responses were compared with the predicted values as shown in Table 7 to validate the method. In this case, the observed values of Q5, Q8 and Q14 were in a very close agreement to the predicted values of optimization. By this method, the validity of the optimization procedure was proven. Optimized conditions were obtained by setting constraints on the dependent and independent variables.

The FTIR spectral analysis of quercetin, pure drug showed that, the principal peaks were observed at wavenumbers of 3924.49, 3833.49, 3709.01, 3562.85, 3438.73, 3396.27, 3289.33, 3094.98, 2989.59, 2907.70, 2780.04, 2579.36, 2392.79, 2313.71, 2203.03, 2079.86, 1968.38, 1797.25, 1679.03, 1488.80, 1438.85, 1280.68, 1198.58, 1048.68, 843.81, 813.89, 670.21, 573.66, and 477.97 (unit in cm-1).The spectra of pure PLGA showed the peaks at wavenumber of 3965.35, 3797.27, 3711.05, 3659.47, 3575.14, 3528.92, 3426.66, 3274.94, 3211.04, 3172.31, 2925.40, 2794.19, 2560.70, 2393.03, 2358.15, 2102.90, 1994.93, 1795.20, 1516.13, 1430.40, 1256.15, 1172.75, 1025.36, 922.95, 765.32, 666.29, 572.65 and 471.88 (unit in cm-1). The spectra of physical mixture of Quercetin and PLGA showed the peaks at wavenumbers of 3935.59, 3842.61, 3631.71, 3527.12, 3417.05, 3311.23, 3215.90, 3051.64, 2811.71, 2561.16, 2465.14, 2316.07, 2184.61, 2101.94, 1953.63, 1780.33, 1461.21, 1279.85, 1153.05, 1039.68, 844.15, 816.46, 669.22 and 566.51 (unit in cm-1). The spectra of quercetin nanoparticle product showed the peaks at wavenumbers of 3890.40, 3756.61, 3626.48, 3540.88, 3438.34, 3385.99, 3299.49, 3218.74, 3097.47, 2952.96, 2851.91, 2566.61, 2341.73, 2212.61, 2110.34, 2016.48, 1790.41, 1751.72, 1573.42, 1445.90, 1264.43, 1165.35, 1063.72, 948.30, 819.23, 686.75, 573.58 and 453.10 (unit in cm-1). The FTIR studies of physical mixture of drug and polymer does not show any significant changes. Thus, these results indicate that there is no interaction between drug and selected polymer. All the FTIR results are shown in Figure 29, 30, 31 and 32.

**Table-7: Optimized values obtained by the constraints applies on R1 to R4**

| **Independent variables** | **Value** | **Predicted values** | | | | **Code** | **Observed values** | | | |
|---|---|---|---|---|---|---|---|---|---|---|
| | | **P. size (R1)** | **Polydisersity index (R2)** | **Entrapment efficiency (R3)** | **CDR After 24 hrs (R4)** | | **P. size (R1)** | **Polydisersity index (R2)** | **Entrapment Efficiency (R3)** | **CDR After 24 hrs (R4)** |
| Drug (Qu) | 15mg | 253.14 | 0.125 | 68.61 | 56.55 | Q5 | 253.11 | 0.121 | 68.59 | 56.50 |
| PLGA | 75mg | | | | | Q8 | 253.10 | 0.124 | 68.63 | 56.52 |
| PVA solution | 2% | | | | | Q14 | 253.14 | 0.122 | 68.65 | 56.54 |

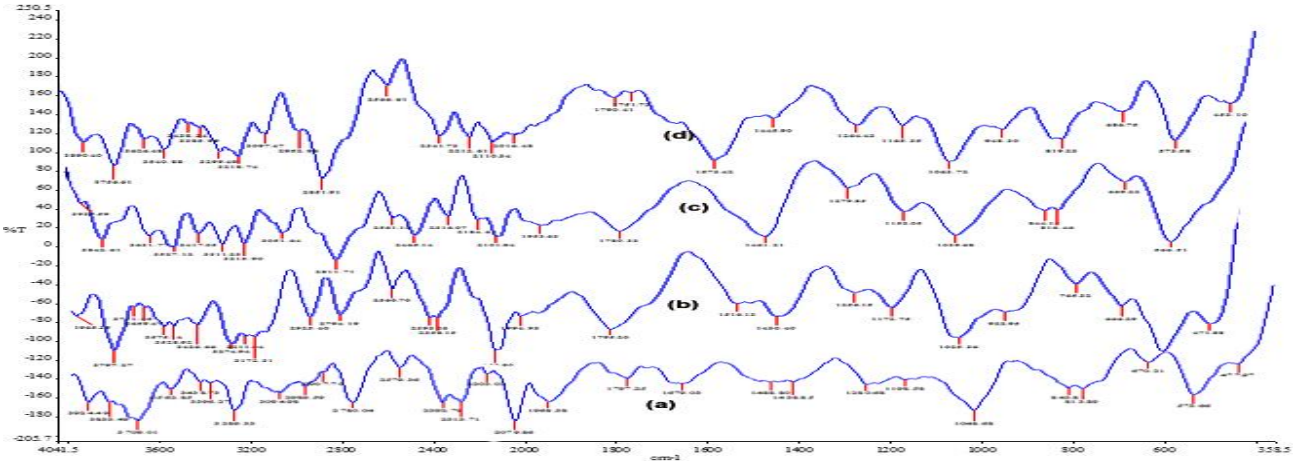


**Figure-9: (a) FTIR spectra of quercetin. (b) FTIR spectra of PLGA. (c) FTIR spectra of quercetin and PLGA. (d) FTIR spectra of quercetin nanoparticle.**

## CONCLUSION

Quercetin-loaded PLGA nanoparticles were successfully prepared by single emulsion solvent evaporation technique. There were three important factors such as variation in drug; polymer and PVA concentration on the influence of four responses including particle size, polydispersity index, entrapment efficiency and cumulative drug release were clearly observed. Numerical optimization using the desirability approach was employed to achieve the desired responses. The observed values of Q5, Q8 and Q14 were in a very close agreement to the predicted values of optimization.

## REFERENCES

[1] S Bosea, Y Du, P Takhistov, BM Kohn. Formulation optimization and topical delivery of quercetin from solid lipid based nanosystems. *International Journal of Pharmaceutics*.441 (2): 56-66 (2013).

[2] A Gupta, K Birhman, I Raheja, SK Sharma, HK Kar. Quercetin: A wonder bioflavonoid with therapeutic potential in disease management. *Asian Pacific Journal of Tropical Disease*.6(3):248-252 (2016).

[3] MK Anwer, MA Al-Mansoor, S Jamil, R Al-Shdefat, MN Ansari, F Shakeel. Development and evaluation of PLGA polymer based nanoparticles of quercetin. *International Journal of Biological Macromolecules*.92: 213–219 (2016).

[4] A Shabir, F Alhusban, Y Perrie, AR Mohammed. Effects of ball-milling on PLGA polymer and its implication on lansoprazole-loaded nanoparticles. *Journal of Basic and Clinical Pharmacy*.2 (2): 71(2011).

[5] A Mohamed. Akl, Alma Kartal-Hodzic, Timo Oksanen, R Hatem. Ismael, M Mohsen. Afouna, Marjo Yliperttula, M Ahmed. Samy, Tapani Viitala. Factorial design formulation optimization and in vitro characterization of curcumin-loaded PLGA nanoparticles for colon delivery. *Journal of Drug Delivery Science and Technology*. 32: 10-20 (2016).

[6] M Mir, N Ahmed, A Ur Rehman. Recent applications of PLGA based nanostructures in drug delivery. *Colloids and Surfaces B: Biointerfaces*. 1(159): 217-31(2017).

[7] Shweta Sharma, Ankush Parmar, Shivpoojan Kori, Rajat Sandhir. PLGA-based nanoparticles: A new paradigm in biomedical applications. *Trends in Analytical Chemistry*.80: 30-40 (2016).

[8] J Jeevanandam, Y San Chan, MK Danquah. Nano-formulations of drugs: recent developments impact and challenges. *Biochimie*.128: 99-112 (2016).